RSC Advances

ROYAL SOCIETY OF CHEMISTRY

www.rsc.org/advances

Journal Name RSCPublishing

ARTICLE

Cite this: DOI: 10.1039/x0xx00000x

Received 00th January 2012,
Accepted 00th January 2012

DOI: 10.1039/x0xx00000x

www.rsc.org/

High-molecular-weight and polar acrylate block copolymers as high-performance dismantlable adhesive materials in response to photoirradiation and postbaking

Tadashi Inui,[a] Eriko Sato[a]* and Akikazu Matsumoto[b]*

We synthesized high-molecular-weight acrylate block copolymers as high-performance dismantlable adhesives consisting of a poly(*tert*-butyl acrylate) (PTBA) sequence as the reactive segment and a random copolymer sequence of *n*-butyl acrylate (nBA) or 2-ethylhexyl acrylate (2EHA) with 2-hydroxyethyl acrylate (HEA) as the adhesive segment using an organotellurium-mediated living radical polymerization (TERP). The adhesion strength of the PtBA/P2EHA and PtBA/PnBA block copolymers containing polar HEA repeating units in their soft segments was high enough to be used as pressure-sensitive adhesives. A quick change in the adhesion property was observed in response to the external dual stimuli of photoirradiation and postbaking during the dismantling process. We discussed the adhesion strength and the failure mode depending on the content of the HEA repeating unit, the sequence structures of the copolymers, and the external stimulus conditions.

Introduction

Reactive and stimuli-responsive polymers with specific functions are used in various application fields.[1-6] Dismantlable adhesion using functional polymers[7-13] is one of practical applications for green sustainable materials and technologies for recycling, rework, and repair systems to save resources, materials, and energies during the manufacturing of industrial and commercial products; for examples, the induction heating using hot-melt polymers,[14] forming using heat-expansive microcapsules,[15,16] and UV- and heat-responsible adhesives.[17-22] Both reliable adhesive strength during use and on-demand easy debonding are required for dismantlable adhesion systems. We previously reported a dismantlable system using degradable polymers containing scissible peroxy bonds in the main chain of the linear polymers or at the cross-linking points of polymer gels.[23-26] A drastic change in the adhesion property was observed for these peroxide-containing polymers in response to either heat or UV irradiation, but it was difficult to simultaneously achieve both stability during use and on-demand quick debonding. Therefore, we proposed a new adhesion system using acrylate block copolymers consisting of a reactive polymer segment and an adhesive polymer segment, which were prepared by living radical polymerization techniques.[27-29] The block copolymers were composed of a poly(*tert*-butyl acrylate) (PtBA) sequence as the reactive polymer segment and any other polyacrylate sequence with a low glass transition temperature (T_g), such as poly(*n*-butyl acrylate) (PnBA) and poly(2-ethylhexyl acrylate) (P2EHA), as the adhesive polymer segment. The former sequence was readily transformed into a poly(acrylic acid) sequence in response to the dual external stimuli of photoirradiation and postbaking in the presence of a photoacid generator,[30-34] while no change occurred in the polymer structures under the conditions using the single stimulus of either photoirradiation or heating. Most polymer materials practically used as pressure-sensitive adhesives include a functional side group, such as the 2-hydroxyethyl acrylate (HEA) repeating unit, which functions as the reacting site in the presence of a cross-linker, in order to increase the adhesive strength, suppress any undesirable deformation at the high temperature, and control the failure characteristics for the practical use of adhesive tapes.[35] The organotellurium-mediated living radical polymerization (TERP) method is one of the most useful methods for the production of high-molecular-weight polyacrylates with unprotected functional side groups.[36-43] In this study, we prepared block copolymers using the TERP method to evaluate the adhesion property of the high-molecular-weight acrylate block copolymers containing polar HEA repeating units. We investigated the adhesion property of the obtained copolymers as the pressure-sensitive adhesive materials under various conditions and their failure characteristics during the dismantling process depending on the content of the HEA repeating unit, the sequence structures, and the photoirradiation and heating conditions as the external stimuli.

Experimental

General Procedure.

The NMR spectra were recorded using a Bruker AV300 spectrometer in chloroform-*d* as the solvent. The FT-IR spectra were recorded using a JASCO FT/IR 430 spectrometer. The number- and weight-average molecular weights (M_n and M_w, respectively) and the polydispersity (M_w/M_n) were determined by size exclusion chromatography (SEC) in tetrahydrofuran as the eluent using a Tosoh CCPD RE-8020 system and calibration with standard polystyrenes. The differential scanning calorimetric (DSC) analysis was performed using a Seiko EXSTAR6200 at the heating rate of 20 °C/min. The atomic force microscopy (AFM) images were taken using a NanoScope IIIa system (Digital Instruments/Veeco) with a cantilever (OMCLAC240TS-C2, Olympus, spring constant 2 N/m,

[a] *Department of Applied Chemistry and Bioengineering, Graduate School of Engineering, Osaka City University, 3-3-138 Sugimoto, Sumiyoshi-ku, Osaka 558-8585, Japan. E-mail: sato@a-chem.eng.osaka-cu.ac.jp; Fax: +81-6-6605-2982; Tel: +81-6-6605-2982*

[b] *Department of Applied Chemistry, Graduate School of Engineering, Osaka Prefecture University, 1-1 Gakuen-cho, Naka-ku, Sakai-shi, Osaka 599-8531, Japan. E-mail: matsumoto@chem.osakafu-u.ac.jp; Fax: +81-72-254-9292; Tel: +81-72-254-9292*

resonant frequency 70 kHz) in the height and phase modes. The samples for the AFM measurements were prepared on a release paper on which the adhesive polymer in acetone (15 wt%) was coated with a thickness of 200 μm, then dried overnight under reduced pressure at room temperature.

Materials.

The acrylate monomers, *tert*-butyl acrylate (tBA), *n*-butyl acrylate (nBA), 2-ethylhexyl acrylate (2EHA), and HEA, were purchased from Tokyo Chemical Industry Co., Ltd., Tokyo, or Wako Pure Chemicals Co., Ltd., Osaka, and distilled before use. 2,2'-Azobis(4-methoxy-2,4-dimethylvaleronitrile) (AMVN) was purchased from Wako Pure Chemicals Co., Ltd., Osaka, and recrystallized from methanol. The commercially available *N*-hydroxynaphthalimide triflate (NIT, 99%, Sigma-Aldrich Co.) was used as received. All the solvents were distilled before use. Ethyl 2-(*n*-butyltellanyl)-2-methylpropionate was synthesized according to the method described in the literature.[39]

Polymerization.

A typical procedure for the TERP using the organomonotelluride chain transfer agent to synthesize the block copolymers is as follows. To a 10-mL glass tube, tBA (1.71 g) and AMVN (0.93 mg) in 3.4 g of ethyl acetate were added and the solution was stirred by argon bubbling at 0 °C for 30 min, followed by the addition of ethyl 2-(*n*-butyltellanyl)-2-methylpropionate (3.4 μL) using a syringe. The polymerization was carried out at 50 °C for 2 h. The conversion, M_n, and M_w/M_n values of the precursor PtBA were determined to be 75.9%, 9.32×10^4 and 1.30, respectively, after the first-stage polymerization. The block copolymerization was carried out at 50 °C for 4 h by the addition of 2EHA (5.66 g) and HEA (0.23 g). The copolymer was separated using a methanol-water mixture (90/10 in volume ratio) as the precipitant. The total conversion of tBA was 86.7%. The conversions of 2EHA and HEA were 45.8 and 52.2%, respectively. The M_n and M_w/M_n values of the resulting block copolymer, PtBA-*b*-P(tBA-*co*-2EHA-*co*-HEA), were 2.58×10^5 and 1.49, respectively. The other block copolymers, PtBA-*b*-P(tBA-*co*-2EHA) and PtBA-*b*-P(tBA-*co*-nBA-*co*-HEA), and the random copolymers, P(tBA-*co*-2EHA-*co*-HEA) and P(tBA-*co*-nBA-*co*-HEA), were similarly synthesized.

Adhesion Properties.

The adhesion test was performed according to the standard test method for the peel adhesion of pressure-sensitive tape (ASTM D3330) using a Tokyo Testing Machine (TTM) universal testing machine, LSC-1/30, with a 1 kN (at maximum) load cell. The 180° peel test was carried out at the peel rates of 30 and 300 mm/min. The adhesive polymers (15 wt%) with 0.4 mol% of NIT as the photoacid generator toward the *tert*-butyl group of the polymers in toluene were coated to a thickness of 200 μm on a poly(ethylene terephthalate) (PET) film (50 μm thickness) using a film applicator, then dried overnight under reduced pressure at room temperature. A 2-cm wide strip of the PET film coated with the adhesive polymers was placed on a stainless steel plate (SUS430, 50 mm × 150 mm × 0.5 mm), then pressed using a 2-kg hand roller. The 180° peel test was carried out after the specimen was left to stand for over 30 min at the determined temperature. For the UV irradiation, the test piece was placed at a distance of 10 cm from the UV source (Toshiba SHL-100UVQ-2) at room temperature. For the thermal treatment, the test piece was placed in a preheated oven, removed from the oven, then naturally cooled to room temperature. The average value of three measurements for the peel test was typically recorded. For the 90° peel creep test, a poly(methyl methacrylate) plate was used as the substrate with an applied 100-g weight to the adhesion area of 10 mm (width) × 50 mm (length) and a holding time until the break down of the test piece was recorded.

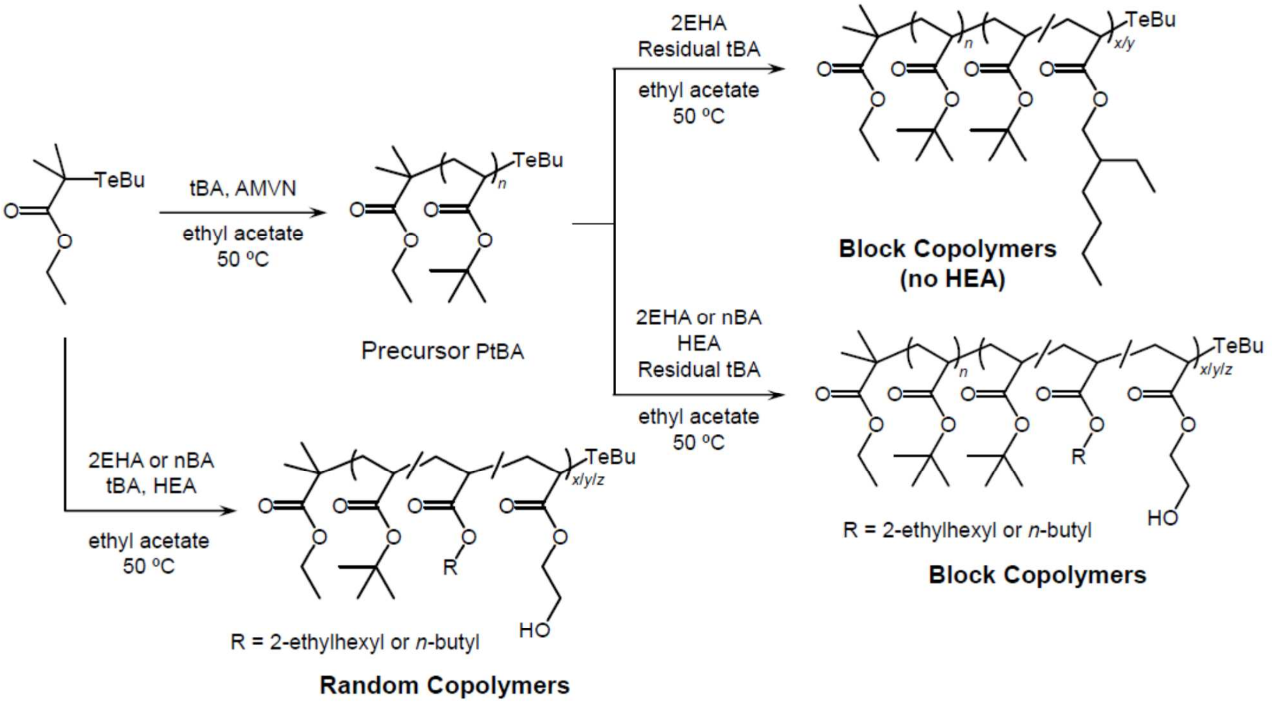

Scheme 1 Synthesis of block and random copolymers by TERP method.

Table 1 Results for the preparation of block and random copolymers by TERP[a]

	For precursor PtBA synthesis						For block or random copolymer syntheses					
		Time	Conv	$M_{n,th}$	M_n			Time	Conv (%)	$M_{n,th}$	M_n	
Code	tBA[b]	(h)	(%)	/10^4	/10^4	M_w/M_n	2EHA/nBA/HEA[b]	(h)	tBA/2EHA/nBA/HEA	/10^5	/10^5	M_w/M_n
Block copolymer synthesis												
2EHA-B0-I	400	2	91.3	4.71	4.47	1.24	1200/−/−	7	94.6/60.0/–/–	1.81	1.60	1.31
2EHA-B0-II	1000	2	83.7	10.8	7.89	1.22	1700/−/−	8	95.0/72.3/–/–	3.49	2.11	1.43
2EHA-B0-III	1000	2	87.0	11.2	9.75	1.24	1000/−/−	8	95.7/71.5/–/–	2.55	1.53	1.26
2EHA-B32	220	2	49.6	1.43	1.57	1.21	2680/−/890	6	62.2/42.4/–/58.2	2.87	2.53	1.56
2EHA-B19	820	2	79.3	10.2	7.38	1.28	1750/−/500	7	82.0/49.0/–/58.0	2.78	2.65	1.74
2EHA-B10	830	2	72.5	7.74	6.18	1.26	1960/−/340	6	81.2/33.7/–/42.3	2.25	1.40	1.40
2EHA-B8	920	2.5	67.7	8.02	7.37	1.28	2180/−/280	4	84.5/45.3/–/50.3	2.98	2.04	1.49
2EHA-B4	890	2	75.9	8.69	9.32	1.30	2050/−/130	4	86.7/45.8/–/52.2	2.80	2.58	1.49
nBA-B15	530	2	78.7	5.37	7.38	1.26	2350/−/510	3	89.5/42.2/–/48.5	2.17	2.66	2.14
nBA-B4	620	2	74.1	5.92	6.86	1.32	2420/−/110	12	89.5/59.8/–/62.0	2.65	2.39	1.48
Random copolymer synthesis												
2EHA-R19	tBA/2EHA/nBA/HEA= 970/1100/–/420							2	76.8/73.4/–/80.6	2.84	2.86	2.03
2EHA-R4	tBA/2EHA/nBA/HEA= 1100/1210/–/100							2	77.8/74.7/–/72.8	2.86	2.35	1.37
nBA-R14	tBA/2EHA/nBA/HEA= 950/–/1560/360							4	76.7/–/75.8/78.8	2.78	2.53	1.88
nBA-R4	tBA/2EHA/nBA/HEA= 740/–/129070							5	90.8/–/90.0/90.3	2.42	2.77	1.67

[a] Polymerization conditions: tBA/solvent = 1/1 in weight in ethyl acetate at 50 °C. The monomer amounts indicate the relative molar ratios to the organomonotelluride. [telluride]/[AMVN] = 1/0.2. The polymerization of tBA was carried out for 2–5 h at the first stage, and then nBA, 2EHA, and HEA were added (monomers/solvent = 1/1 in weight). The theoretical number-average molecular weight ($M_{n,th}$) was calculated based on the monomer conversions. [b] Molar ratio to the monotelluride.

Results and discussion

Synthesis of Copolymers.

The block copolymers consisting of the reactive PtBA segment and the adhesive P2EHA or PnBA segment were synthesized by the TERP method using an organomonotelluride compound as the chain transfer agent. Scheme 1 shows the reactions used for the synthesis of the 2EHA block copolymers in the absence and presence of HEA. The polymerization results are shown in Table 1. The second monomers were added to the polymerization solution after the first-step polymerization of tBA without isolating the produced PtBA precursor. As a result, the soft segment of the block copolymers consisted of the random copolymer sequences of several monomers including a small amount of the residual tBA. Similarly, the random copolymers were synthesized by the one-step polymerization procedure (Scheme 1 and Table 1).

The high-molecular-weight block copolymers with a well-controlled molecular weight distribution were produced in the absence of HEA (the **2EHA-B0**s, M_n = 1.5−2.1 × 10^5, M_w/M_n = 1.26−1.43). The block copolymers with a high M_w value were similarly produced during the copolymerization in the presence of HEA (**2EHA-B32** to **2EHA-B4**, M_n = 1.4−2.7 × 10^5). The M_w/M_n values increased when the block copolymers had a high HEA content and a high molecular weight, as shown in the SEC curves in Fig. 1. Similar results were also observed for random copolymerizations in the presence of HEA. This was due to the frequent chain transfer to the HEA repeating units under the conditions that provided a high-molecular-weight block copolymer including HEA repeating units in a high content because of a free radical propagation mechanism.

In this study, the weight fractions of each component contained in the copolymers were optimized by considering the entire hardness of the copolymers as the adhesives under the room temperature conditions. The sequence structure, the M_w and M_w/M_n values, the weight fractions of each component, and the T_g values are summarized in Table 2. It was confirmed by the DSC measurement that the T_g values were observed in the ranges of −67 to −53 °C and −46 to −39 °C for the P2EHA and PnBA block segments, respectively, and 42−43 °C as the constant value for the PtBA segment. In the case of 2EHA-B32, the PtBA segment was too short to show its T_g on the DSC trace. In contrast, intermediate and single

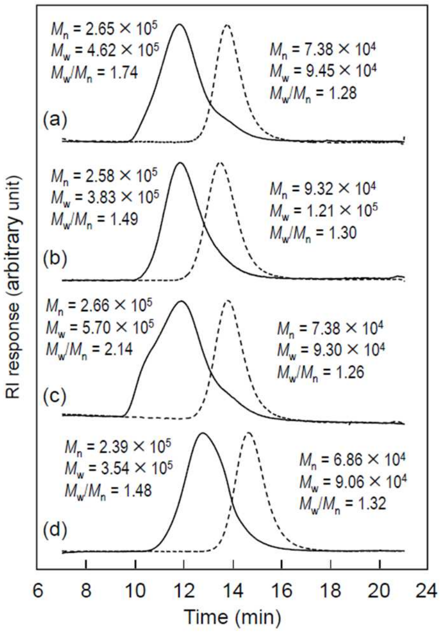

Fig. 1 SEC traces of the precursor PtBA (dotted curves) and the block copolymers (solid curves) for the synthesis of (a) **2EHA-B19**, (b) **2EHA-B4**, (c) **nBA-B15**, and (d) **nBA-B4**.

Table 2 Structure and characterization of high-molecular-weight block and random copolymers used in this study

Abbreviation	Polymer structure[a]	$M_w/10^5$	M_w/M_n	Weight fraction (wt%) tBA/2EHA/nBA/HEA	T_g[b] (°C)
2EHA-B0-I	PtBA$_{35.9}$-*b*-P(tBA$_{1.3}$-*co*-2EHA$_{62.8}$)	2.10	1.31	29.2/70.8/−/−	−67, 42
2EHA-B0-II	PtBA$_{39.4}$-*b*-P(tBA$_{3.6}$-*co*-2EHA$_{57.0}$)	3.02	1.43	34.4/65.6/−/−	[c]
2EHA-B0-III	PtBA$_{51.0}$-*b*-P(tBA$_{7.3}$-*co*-2EHA$_{41.7}$)	1.93	1.26	49.3/50.7/−/−	[c]
2EHA-B32	PtBA$_{3.3}$-*b*-P(tBA$_{1.5}$-*co*-2EHA$_{63.2}$-*co*-HEA$_{32.0}$)	3.95	1.56	3.9/72.9/−/23.3	−54
2EHA-B19	PtBA$_{33.4}$-*b*-P(tBA$_{1.1}$-*co*-2EHA$_{47.0}$-*co*-HEA$_{18.5}$)	4.62	1.74	29.0/56.9/−/14.1	−53, 42
2EHA-B10	PtBA$_{40.7}$-*b*-P(tBA$_{4.9}$-*co*-2EHA$_{44.5}$-*co*-HEA$_{9.9}$)	1.40	1.40	38.5/54.0/−/7.6	[c]
2EHA-B8	PtBA$_{28.1}$-*b*-P(tBA$_{8.3}$-*co*-2EHA$_{55.3}$-*co*-HEA$_{8.3}$)	3.03	1.82	31.9/61.5/−/6.6	[c]
2EHA-B4	PtBA$_{37.8}$-*b*-P(tBA$_{5.4}$-*co*-2EHA$_{52.5}$-*co*-HEA$_{4.3}$)	3.83	1.49	35.2/61.6/−/3.2	−61, 43
nBA-B15	PtBA$_{28.7}$-*b*-P(tBA$_{4.0}$-*co*-nBA$_{52.3}$-*co*-HEA$_{14.9}$)	5.70	2.14	33.2/−/53.1/13.7	−39, 43
nBA-B4	PtBA$_{24.1}$-*b*-P(tBA$_{5.0}$-*co*-nBA$_{67.0}$-*co*-HEA$_{3.9}$)	3.54	1.48	29.2/−/67.2/3.6	−46, 43
2EHA-R19	P(tBA$_{38.7}$-*co*-2EHA$_{42.1}$-*co*-HEA$_{19.2}$)	5.80	2.03	33.2/51.9/−/14.9	−31
2EHA-R4	P(tBA$_{47.8}$-*co*-2EHA$_{48.4}$-*co*-HEA$_{3.7}$)	3.21	1.37	39.6/57.6/−/2.8	−34
nBA-R14	P(tBA$_{33.1}$-*co*-nBA$_{53.0}$-*co*-HEA$_{13.9}$)	4.75	1.88	33.5/−/53.7/12.8	−21
nBA-R4	P(tBA$_{35.5}$-*co*-nBA$_{60.8}$-*co*-HEA$_{3.7}$)	4.63	1.67	35.6/−/61.1/3.4	−25

[a] The subscript numbers denote the molar fraction of each monomer unit. [b] Determined by DSC. [c] Not determined.

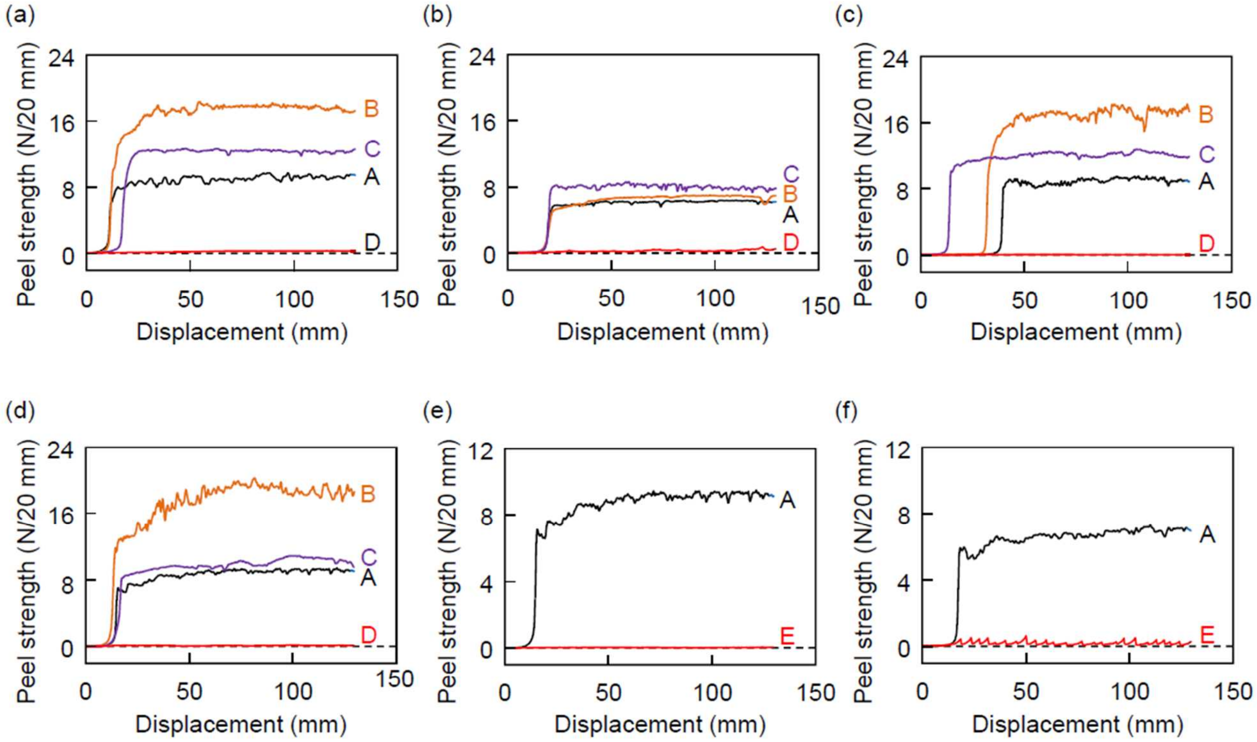

Fig. 2 Representative peel strength-displacement curves of (a) **2EHA-B19**, (b) **2EHA-B4**, (c) **nBA-B15**, (d) **nBA-B4,** (e) **nBA-B15** and (f) **nBA-R14** with 0.4 mol% of NIT. Stimuli conditions: A, before irradiation and heating; B, after heating at 100 °C for 1 h; C, after UV irradiation for 1 h; D, after UV irradiation for 1 h and postbaking at 100 °C for 1 h; and E, after preheating at 100 °C for 1 h and the subsequent UV irradiation for 1 h followed by postbaking at 100 °C for 1 h. Tape width, 20 mm; peel rate, 30 mm/min.

T_g values for the random copolymers were observed in the temperature range of −34 to −21 °C. The copolymers with M_w values greater than 10^5, optimized comonomer compositions, and controlled block sequences were favourably used as the adhesive materials in this study.

Adhesion Properties of 2EHA Block Copolymers.

The adhesive properties were first investigated using the 2EHA block copolymers containing no HEA unit with different composition ratios for the hard and soft segments. Because the **2EHA-B0-III** with the highest tBA content was too hard to exhibit the required adhesion property, we carried out the 180° peel tests using two other samples. The photoirradiation and heating conditions as the external stimuli for dismantling, i.e., 1-h UV irradiation and 1-h postbaking at 100 °C, were selected as the conditions sufficient enough to induce the quantitative transformation of the tBA repeating units to the acid form based on the previous results.[27-29] The adhesion strength of **2EHA-B0-I** was

Table 3 Peel strength of acrylate block copolymers used as the dismantlable adhesives in the presence of NIT as the photoacid generator under various conditions[a]

Adhesive	Sequence structure	Stimuli conditions[b]	Peel strength (N/20 mm)	Relative value	Failure mode
2EHA-B0-I	$PtBA_{35.9}$-*b*-P($tBA_{1.3}$-*co*-$2EHA_{62.8}$)	A	0.31	1	cohesive
		D	0.36	1.15	cohesive
2EHA-B0-II	$PtBA_{39.4}$-*b*-P($tBA_{3.6}$-*co*-$2EHA_{57.0}$)	A	1.26	1	cohesive
		D	0.79	0.62	cohesive
2EHA-B32	$PtBA_{3.3}$-*b*-P($tBA_{1.5}$-*co*-$2EHA_{63.2}$-*co*-$HEA_{32.0}$)	A	5.6 ± 0.7	1	SUS-interfacial
		D	0.16 ± 0.08	0.03	PET-interfacial
2EHA-B19	$PtBA_{33.4}$-*b*-P($tBA_{1.1}$-*co*-$2EHA_{47.0}$-*co*-$HEA_{18.5}$)	A	9.2 ± 1.2	1	SUS-interfacial
		B	18.0 ± 1.2	1.96	cohesive
		C	12.9 ± 0.5	1.40	SUS-interfacial
		D	~0	~0	PET-interfacial
		E	~0	~0	PET-interfacial
2EHA-B10	$PtBA_{40.7}$-*b*-P($tBA_{4.9}$-*co*-$2EHA_{44.5}$-*co*-$HEA_{9.9}$)	A	2.4 ± 1.2	1	SUS-interfacial
		D	~0	~0	PET-interfacial
2EHA-B8	$PtBA_{28.1}$-*b*-P($tBA_{8.3}$-*co*-$2EHA_{55.3}$-*co*-$HEA_{8.3}$)	A	8.3	1	SUS-interfacial
		B	11.9	1.43	cohesive
		C	9.6	1.15	SUS-interfacial
		D	0.09	0.01	cohesive
2EHA-B4	$PtBA_{37.8}$-*b*-P($tBA_{5.4}$-*co*-$2EHA_{52.5}$-*co*-$HEA_{4.3}$)	A	6.0 ± 0.3	1	SUS-interfacial
		B	7.0 ± 1.2	1.17	cohesive
		C	8.9 ± 0.8	1.47	SUS-interfacial
		D	0.35 ± 0.19	0.06	cohesive
nBA-B15	$PtBA_{28.7}$-*b*-P($tBA_{4.0}$-*co*-$nBA_{52.3}$-*co*-$HEA_{14.9}$)	A	7.6 ± 2.5	1	SUS-interfacial
		B	17.2 ± 0.8	2.25	SUS-interfacial
		C	12.2 ± 1.0	1.59	SUS-interfacial
		D	~0	~0	PET-interfacial
		E	~0	~0	PET-interfacial
nBA-B4	$PtBA_{24.1}$-*b*-P($tBA_{5.0}$-*co*-$nBA_{67.0}$-*co*-$HEA_{3.9}$)	A	9.0 ± 0.9	1	SUS-interfacial
		B	18.5 ± 0.3	2.06	cohesive
		C	10.3 ± 0.2	1.15	SUS-interfacial
		D	0.07 ± 0.02	0.01	PET-interfacial
2EHA-R14	P($tBA_{38.7}$-*co*-$2EHA_{42.1}$-*co*-$HEA_{19.2}$)	A	9.1	1	SUS-interfacial
		B	12.2	1.34	cohesive
		C	12.4	1.36	SUS-interfacial
		D	stick slip	–	–
2EHA-R4	P($tBA_{47.8}$-*co*-$2EHA_{48.4}$-*co*-$HEA_{3.7}$)	A	9.2	1	SUS-interfacial
		B	14.2	1.54	cohesive
		C	7.8	0.85	SUS-interfacial
		D	stick slip	–	–
nBA-R14	P($tBA_{33.1}$-*co*-$nBA_{53.0}$-*co*-$HEA_{13.9}$)	A	6.5 ± 1.6	1	SUS-interfacial
		B	15.7 ± 2.6	2.39	cohesive
		C	8.4 ± 0.4	1.28	SUS-interfacial
		D	stick slip	–	–
		E	stick slip	–	–
nBA-R4	P($tBA_{35.5}$-*co*-$nBA_{60.8}$-*co*-$HEA_{3.7}$)	A	6.9 ± 0.7	1	SUS-interfacial
		B	16.9 ± 3.7	2.43	cohesive
		C	7.8 ± 0.3	1.13	SUS-interfacial
		D	stick slip	–	–

[a] NIT (0.4 mol% relative to tBA units) was used as the photoacid generator. Tape width, 20 mm; peel rate, 30 mm/min; peel temperature, 23 °C. [b] A, before irradiation and heating; B, after heating at 100 °C for 1 h; C, after UV irradiation for 1 h; D, after UV irradiation for 1 h and postbaking at 100 °C for 1 h; E, after preheating at 100 °C for 1 h and the subsequent UV irradiation for 1 h followed by postbaking at 100 °C for 1 h.

0.31 N/20 mm was much lower than those of commercial adhesion tapes. The weak coagulation force of the adhesive polymers resulted in a cohesive failure, as shown in Table 3. As the tBA content increased, the average adhesion strength increased to ca. 1 N/20 mm (**2EHA-B0-II**), which was still insufficient to be used as the adhesive tapes. The molecular weight of the 2EHA block copolymers was high enough ($M_w > 10^5$) to be used as the adhesive polymers and the T_g value of the soft segment was as low as –67 °C. Nevertheless, the cohesive force of these polymers was very low. After photoirradiation and heating, no drastic change in the adhesion strength was observed although the chemical transformation of the *tert*-butyl group to the acid was confirmed after the applied dual stimuli. Thus, the required adhesive property was not obtained by the control of the sequence ratio of the block copolymer segments.

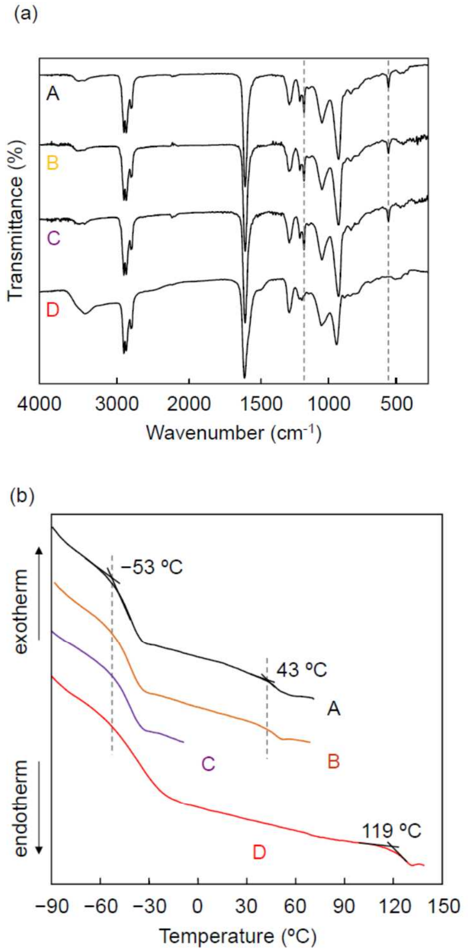

Fig. 3 (a) IR spectra and (b) DSC traces of **2EHA-B19** with 0.4 mol% NIT before and after each treatment by external stimuli. Stimulus conditions: A, Before UV irradiation and heating; B, after heating at 100 °C for 1 h; C, after UV irradiation for 1 h; D, after UV irradiation for 1 h and postbaking at 100 °C for 1 h.

Next, the adhesive property was investigated for the block copolymers of which the soft segment contained the polar HEA repeating unit. The contents of the HEA unit were 4.3–32.0 mol%, which corresponded to 3.2–23.3 wt% for the 2EHA block copolymers, as shown in Table 2. The results of the 180° peel test for **2EHA-B19** and **2EHA-B4**, which contained 18.5 and 4.3 mol% of the HEA units, respectively, are shown in Fig. 2(a) and (b). The adhesive properties and the failure mode for the 2EHA block copolymers with different HEA contents are summarized in Table 2. The adhesion strength of the tapes using the block copolymers containing the HEA units was much higher than that for the copolymers without HEA units. The failure mode was interfacial failure at an interface between the polymers and a stainless steel (SUS) plate. The introduction of the HEA units was expected to increase both the cohesive force and interface interactions. The cohesive force was actually greater than the adhesive forces at the interfaces, leading to the selective interfacial failure mode during the peeling test.

After one heating of the **2EHA-B19** adhesive tape at 100 °C for 1 h (condition B in Fig. 2), the adhesion strength at room temperature increased to twice that before heating and the failure mode changed to a cohesive one. The failure mode depends on the magnitude and the balance of the cohesive force of the adhesive polymer and the interfacial adhesive force between the adhesive polymer and the adherend. The smallest force determines the entire failure mode of the used adhesive system. An increase in the adhesion strength observed during heating the **2EHA-B19** system was due to an increase in the intermolecular interaction between the SUS surface and the hydroxy group contained in the HEA repeating units. As a result, the adhesion strength depended on the polymer cohesive force due to the higher adhesive force at the interface. The adhesion strength slightly increased and the interfacial failure was observed at the polymer-SUS interface after photoirradiation without postbaking (condition C in Fig. 2), due to the occurrence of a partial cross-linking.

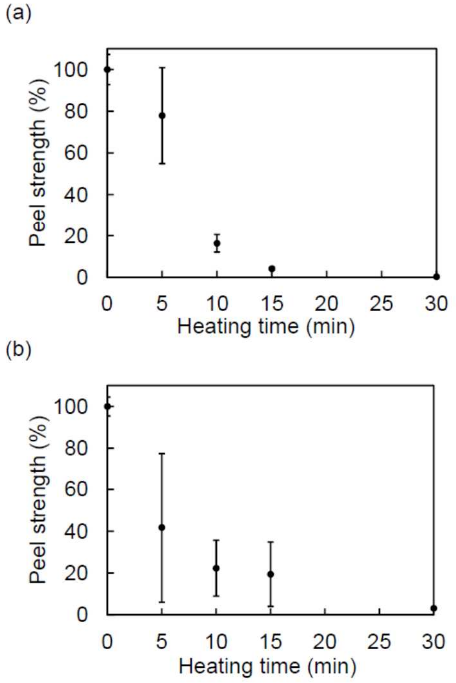

Fig. 4 Relative peel strength of (a) **nBA-B15** and (b) **nBA-R14** after UV irradiation for 1 h and postbaking at 100 °C for 0 to 30 min.

The adhesion strength significantly decreased after photoirradiation and postbaking by a change in the structure of the polymer side group in the PtBA segment (condition D in Fig. 2). The failure mode was interfacial failures at the PET side except for the case of the polymers with low HEA contents**,** which exhibited a cohesive failure. This indicated a significant increase in a cohesive force of the adhesives with a high HEA content. During the dismantling process by the dual external stimuli, isobutene gas evolution and partial polymer cross-linking were observed. Fig. 3(a) shows the changes in the IR spectra of the polymer adhesives before and after the photoirradiation and heating. These spectra revealed that no change occurred after either the photoirradiation or heating, while complete disappearance of the peak characteristic of the *tert*-butyl group at 846 cm^{-1} occurred after both the photoirradiation and postbaking. The intensity of the peak due to the methyl group observed at 1170 cm^{-1} also decreased in the spectrum recorded after the photoirradiation and postbaking. It was confirmed that the quantitative transformation of the tBA repeating unit into the carboxylic acid under the conditions of a 1-h photoirradiation and the subsequent heating at 100 °C for 1 h.

Table 4 Effects of polymer sequence and temperature on adhesion property of the copolymers

Adhesive polymer	180° peel strength[a] (N/20 mm)		
	70 °C	23 °C	0 °C
2EHA-B19	6.8 (0.59)	11.5 [9.2][b]	2.0 (0.17)
2EHA-B4	0.8 (0.10)	8.0 [6.0][b]	3.1 (0.39)
nBA-B15	[c]	9.3 [7.6][b]	0.10 (0.01)
nBA-B4	[c]	8.7 [9.0][b]	0.20 (0.02)
2EHA-R19	2.0 (0.23)	8.6 [9.1][b]	2.0 (0.23)
2EHA-R4	0.1 (0.01)	9.0 [9.2][b]	1.6 (0.18)
nBA-R14	4.8 (0.69)	7.0 [6.5][b]	0.32 (0.05)
nBA-R4	0.6 (0.07)	8.1 [6.9][b]	0.65 (0.08)

[a] Tape width, 20 mm; peel rate, 300 mm/min. Values in parentheses indicate the relative peel strength determined at 70 and 0 °C versus that at 23 °C. [b] Values in brackets indicate the data at the peel rate of 30 mm/min (see Table 3). [c] Not determined.

In the DSC traces of the polymers before and after the applied stimuli under similar conditions [Fig. 3(b)], the transition due to the T_g of the PtBA segment at 43 °C disappeared and a new transition was observed at 119 °C after the photoirradiation and postbaking. No change was observed for the T_g values of the soft segment at –53 °C after either photoirradiation or heating. A slight increase in the T_g value was observed after photoirradiation and postbaking due to the change in the small amount of *tert*-butyl group into the acid included in the soft segment (1.1 mol%, see Table 2).

Adhesion Properties of nBA Block Copolymers.

We next investigated the adhesion properties of the nBA block copolymers in comparison with those using the 2EHA block copolymers in order to clarify the role of the soft segments. The results are shown in Table 3 and Fig. 2(c) and (d). The strength values and the SUS-interfacial failure mode of the nBA block copolymers were similar to those of the 2EHA block copolymers. The strength values of **nBA-B4** and **nBA-B15** after heating increased to twice that of the original. The failure mode of the **nBA-B4** changed from the interfacial to the cohesive failure during the heating while no change in the failure mode was observed for **nBA-B15**. This suggested that the adhesive force at the SUS-interface increased to a value higher than the cohesive force during the heating of the test piece using **nBA-B4**. The T_g values of the PnBA segment was determined to be –52 °C by DSC, being higher than that of the P2EHA segment at –70 °C. The cohesive force of the nBA segment as the soft segment of the block copolymers was greater than that of the 2EHA segment even at room temperature.

In order to examine the stability of the adhesive materials against the heat conditions before and during their use, we checked the effect of preheating on the dismantling process. As shown in Fig. 2(e) and (f), the peel strength was determined for the samples, which were preheated at 100 °C for 1 h, then photoirradiated for 1 h, followed by postbaking at 100 °C for 1 h (condition E in Fig. 2). The spontaneous peeling after the photoirradiation and postbaking was achieved independent of the presence and absence of the preheating process. This suggests no deterioration in the adhesive materials during the heating under the conditions at 100 °C for 1 h when they are stored in the dark. This also indicated the importance of the order of the applied stimuli; i.e., a postbaking process after photoirradiation is uniquely valid for the efficient dismantling. In other words, these adhesive materials are tolerant to a change in the thermal conditions during use because they maintain their adhesive strength unless photoirradiated before heating.

Effects of Polymer Sequence Structures.

We also compared the adhesion properties of the systems using the block and random copolymers. The adhesive strength and failure mode of the random copolymers were similar to those of the corresponding block copolymers as the original adhesives without any stimulus, but a decrease in the adhesion strength was insufficient for the random copolymers after the dual stimuli of photoirradiation and postbaking (Table 3). Furthermore, the relative strengths after postbaking at 100 °C for different times of the tapes using **nBA-B15** and **nBA-R14** shown in Fig. 4 indicated that the heating for 10 min was sufficient for **nBA-B15** to decrease the adhesion strength to the less than 20% of that before the photoirradiation and postbaking. For the random copolymers, longer heating was required to decrease their adhesion strength and greater standard deviation was observed [Fig. 4(b)]. The stick-slip peeling behaviour was observed for the adhesive tapes using the random copolymers after photoirradiation and postbaking [Table 3 and Fig. 2(f)]. Thus, the block copolymers had a superior property as the dismantling adhesive materials due to achieving the spontaneous peeling during a shorter postbaking period. The production of foams was observed on the entire part of the adherent layers in the case of the random copolymers, being due to the isobutene gas evolution. In contrast, the isobutene gas was effectively evolved at the interfaces of the adherent and the substrates.

The 180° peel strength values were determined at different temperatures and the results are summarized in Table 4. The data in Table 4 were determined at the peel rate of 300 mm/min. The strength values were higher than those determined at 30 mm/min as shown in Table 3, because the viscoelastic properties of the pressure-sensitive adhesive materials significantly depend on the peel rate. For all the copolymers, the adhesion strength values at 0 and 70 °C were lower when compared to those at 23 °C, because the composition ratios of the repeating monomer units were optimized based on the adhesive properties of the copolymers under the condition of room temperature in this study. The relative strength values were 0.2–0.4 at 0 °C for the 2EHA-containing copolymers, while they were lower than 0.1 for the nBA copolymers. This indicated the high performance of the 2EHA copolymers at a low temperature. The nBA-containing soft segments became harder at a low temperature, resulting in a decrease in the adhesion force at an interface between the adhesives and the SUS as the adherend. Based on the result of the 90° peel creep test using a poly(methyl methacrylate) plate with an applied 100-g weight at 23 °C, it was confirmed that **nBA-B15** and **2EHA-B19** maintained the highest holding powers; i.e., the peel creep distances were less than 50 mm

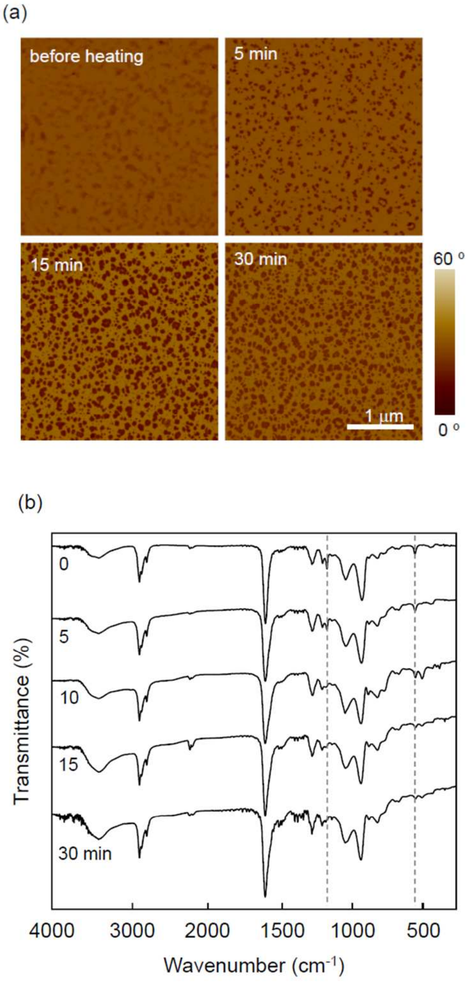

Fig. 5 (a) AFM phase images and (b) IR spectra of **nBA-15B** with 0.4 mol% NIT before and after UV irradiation and the subsequent heating at 100 °C for 5–30 min.

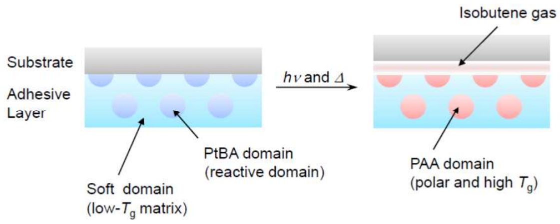

Fig. 6 Illustration of the cross-sections of the adhesive specimens using block copolymer adhesives.

after 3 h, while the test pieces using the block and random copolymers containing an amount of HEA unit less than 4 wt% were readily broken down within 10 min under similar conditions. This was due to a difference in the interfacial adhesive and cohesive forces depending on the content of the polar HEA repeating units. The nBA block copolymers exhibited a property superior to the 2EHA block copolymers for the peel creep experiments. The random copolymers showed a greater creep distance than the corresponding block copolymers.

Dismantling Mechanism.

A change in the surface morphology of the adhesive polymers during the dismantling process after the applied dual stimuli of photoirradiation and postbaking was investigated by AFM observations. In the phase and height images of the block copolymer, microphase separated structures were observed, while no domain structure was observed for the random copolymers before and after the change in the conditions. The phase images of the **nBA-15B** surfaces before and after postbaking are shown in Fig. 5. The areas observed as dark images with a small delay in the phase images correspond to the PtBA domain with a high T_g value. No drastic change was observed in the phase-separated domains during the postbaking, but the contrast became clearer according to the postbaking time. The fraction of the dark domains slightly increased after the longer postbaking. This was due to a change in the chemical structure of the PtBA segment to the poly(acrylic acid) segment, which had a higher T_g value and a polar side group. The IR spectral change of **nBA-15B** in Fig. 5(b) supported the gradual transformation of the *tert*-butyl ester to the carboxylic acid, similar to the results for **2EHA-B19** in Fig. 3(b).

The drastic decrease in the adhesion strength by the change in the side group from the *tert*-butyl ester to the carboxylic acid is due to a decrease in the adhesion area at the interface by the evolution of isobutene gas. The other possible reason is a decrease in the interfacial closeness between the adherent and the substrates by an increase in the elasticity of the adhesive polymers. The latter can be induced by both the increase in the T_g value [Fig. 3(b)] due to the side group transformation and the formation of a partial cross-linking structure by transesterification. The gel formation was confirmed by the solubility test of the adhesive materials recovered after photoirradiation and postbaking. The change in the adhesive property during the dismantling process was more obvious for the block copolymers than for the random copolymers. This was probably because the physical property changed in the entire adhesive layer of the random copolymers during the photoirradiation and postbaking, and consequently, the evolved isobutene gas was trapped in the totally hardened adhesive layer, resulting in the formation of a high number of bubbles in the layers, as shown in a schematic illustration in Fig. 6. In contrast, the soft segment domain of the block copolymers remained their low-T_g values during the side-chain transformation of the hard segment of the block copolymers, and the evolved isobutene readily diffused through the soft domain and reached the interfaces of the substrates. The magnitude of the changes in the T_g values and the elasticity for the hard segment of the block copolymer was much greater than those in the random copolymers.

Conclusions

We demonstrated that the adhesive property of the dismantlable adhesion materials consisting of acrylate block copolymers was significantly modified by the introduction of the polar HEA repeating units into the tBA/2EHA and tBA/nBA block copolymers, which were successfully produced by the TERP method. The obtained block copolymer exhibited excellent adhesive properties as dismantlable adhesion materials; i.e., high adhesion strength values and thermal stability during the use as the adhesive tapes and quick and spontaneous dismantling in response to dual external stimuli consisting of photoirradiation and postbaking. We also revealed the superior dismantling property of the block copolymers during the quick debonding process with a short postbaking time. The double-locked adhesion systems, which selectively respond to only the dual stimuli of photoirradiation and postbaking, will also be applied to various fields related to green sustainable technology to save resources, materials, and energies.

Notes and references

1 P. Schattling, F. D. Jochum and P. Theato, *Polym. Chem.*, 2014, **5**, 25-36.
2 G. L. Fiore, S. J. Rowan and C. Weder, *Chem .Soc. Rev.*, 2013, **42**, 7278-7288.
3 X. -Z. Yan, F. Wang, B. Aheng and F. -H. Huang, *Chem .Soc. Rev.*, 2012, **41**, 6042-6065.
4 B. -W. Xin and J. -C. Hao, *Chem .Soc. Rev.*, 2010, **39**, 769-782.
5 D. Roy, J. N. Cambre and B. S. Sumerlin, *Prog. Polym. Sci.*, 2010, **35,** 278-301.
6 F. Lui and M. W. Urban, *Prog. Polym. Sci.*, 2010, **35,** 3-23.
7 S. Yang, J. -S. Chen, H. Körner, T. Breiner and C. K. Ober, *Chem. Mater.,* 1998, **10**, 1475-1482.
8 M. Shirai, S. Morishita, H. Okamura and M. Tsunooka, *Chem. Mater.,* 2002, **14**, 334-340.
9 A. J. Baldan, *Mater. Sci.,*2004, **39**, 1-49.
10 L. J. Wang, H. Y. Li and C. P. Wong, *J. Polym. Sci., Part A, Polym. Chem.,* 2000, **38**, 3771-3782.
11 J. -S. Chen, C. K. Ober and M. D. Poliks, *Polymer,* 2002, **43**, 131-139.
12 L. González, F. Ferrando, X. Ramis, J. M. Salla, A. Mantecón and A. Serra, *Prog. Org. Coat.*, 2009, **65**, 175-181.
13 A. R. Hutchinson, P. H. Winfield and R. H. McCurdy, *Adv. Eng. Mater.,* 2010, **12**, 646-652.
14 T. Sekine, H. Tomita, S. Obata, and Y. Saito, *Electr. Eng. Jpn.,* 2009, **168**, 32-39.
15 Y. Nishiyama, N. Uto, C. Sato, and H. Sakurai, *Int. J. Adhes. Adhes.,* 2003, **23**, 377-382.
16 H. Ishikawa, K. Seto, S. Shimotuma, N. Kishi, and C. Sato, *Int. J. Adhes. Adhes.,* 2005, **25**, 193-199.
17 K. Ogino, J. -S. Chen and C. K. Ober, *Chem. Mater.*, 1998, **10**, 3833-3838.
18 J. Malik and S. J. Clarson, *Int. J. Adhes. Adhes.,* 2002, **22**, 283-289.
19 M. Shirai, *Prog. Org. Coat.*, 2007, **58**, 158-165.
20 T. Ozawa, S. Ishikawa, Y. Kano and T. Kasemura, *J. Adhesion*, 2000, **72**, 1-16.
21 K. Ebe, H. Seno and K. Horigome, *J. Appl Polym. Sci.*, 2003, **90**, 436-441.
22 S. -W. Lee, J. -W. Park, Y. -H. Lee, H. -J. Kim, M. Rafailovich and J. Sokolov, *J. Adhes. Sci. Technol.*, 2012, **26**, 1629-1643.
23 E. Sato, H. Tamura and A. Matsumoto, *ACS Appl. Mater. Inter.,* 2010, **2**, 2594-2601.
24 E. Sato, T. Hagihara and A. Matsumoto, *ACS Appl. Mater. Inter.*, 2012, **4**, 2057-2064.
25 A. Mihashi, H. Tamura, E. Sato and A. Matsumoto, *Prog. Org. Coat.*, 2010, **67**, 85-91.
26 E. Sato and A. Matsumoto,*Chem. Rec.*, 2009, **9**, 247-257.
27 T. Inui, E. Sato, and A. Matsumoto, *ACS Appl. Mater. Interfaces*, 2012, **4**, 2124-2132.
28 K. Yamanishi, E. Sato and A. Matsumoto, *J. Photopolym. Sci. Technol.*, 2013, **26**, 239-244.
29 T. Inui, K. Yamanishi, E. Sato and A. Matsumoto, *Macromolecules*, 2013, **46**, 8111-8120.
30 Ito, H. *Adv. Polym. Sci.*, 2005, **172**, 37-245.
31 F. Ortica, J. C. Scaiano, G. Pohlers, J. F. Cameron and A. Zampini, *Chem. Mater.,* 2000, **12**, 414-420.
32 H. Okamura, K. Sakai, M. Tsunooka, M. Shirai, T. Fujiki, S. Kawasaki and M. Yamada, *J. Photopolym. Sci. Technol.,* 2003, **16**, 87-90.
33 J. -P. Malval, S. Suzuki, F. Morlet-Savary, X. Allomas, J. -P. Fonassier, S. Takahara, and T. Yamaoka, *J. Phys. Chem. A*, 2008,**112** 3879-3885.
34 H. Okamura and M. Shirai, *Trends Photochem. Photobio.*, 2013, **15**, 51-61.
35 A. I. Everaerts and L. M.Clemens, In *Adhesion Science and Engineering 2, Surfaces, Chemistry & Applications*, eds., M. Chaudhury and A. V. Pocius, Elsevier,:Amsterdam, 2002, Chapter 11, pp. 465-534.
36 S. Yamago, *J. Polym. Sci., Part A,Polym. Chem.,* 2006, **44**, 1-12.
37 S. Yamago, *Chem. Rev.,* 2009, **109**, 5051-5068.
38 S. Yamago and Y. Nakamura, In *Polymer Science: A Comprehensive Reference,* Eds-in-Chief K. Matyjaszewski, Möller, M.; vol. eds., G. W.Coates and M.Sawamoto, Elsevier: Amsterdom, 2012, pp. 227-248.
39 S. Yamago, K. Iida and J. Yoshida, *J. Am. Chem. Soc.,* 2002, **124**, 2874-2875.
40 S. Yusa, S. Yamago, M. Sugahara, S. Morikawa, T. Yamamoto and Y. Morishima, *Macromolecules,* 2007, **40**, 5907-5915.
41 E. Kayahara, S. Yamago, Y. Kwak, A. Goto and T. Fukuda, *Macromolecules,* 2008, **41**, 527-529.
42 M. Okubo, Y. Sugihara, Y. Kitayama, Y. Kagawa and H. Minami, *Macromolecules,* 2009, **42**, 1979-1986
43 Y. Nakamura, T. Arima, S. Tomita and S. Yamago, *J. Am. Chem. Soc.,* 2012, **134**, 5536-5539.

Graphic abstract